EMPLOYING MULTIPLE GEOPHYSICAL SENSOR SYSTEMS TO ENHANCE BURIED UXO "TARGET RECOGNITION" CAPABILITY

Dwain K. Butler*
Alion Science and Technology Corp.
Vicksburg, Mississippi 39180-6199

Donald E. Yule and Hollis H. Bennett, Jr.
U.S. Army Engineer Research and Development Center
Vicksburg, Mississippi 39180-6199

Abstract

Millions of acres of former and currently used military training and testing ranges are potentially contaminated by surface and buried unexploded ordnance (UXO), giving rise to requirements for UXO environmental restoration of formerly used sites and for sustainable use and active range cleanup. Geophysical surveys are required to map the location of buried UXO. The major cost driver of current cleanup and restoration is the inability to discriminate between buried false alarm and UXO targets. Excavation of false alarm targets is the major cost driver of UXO cleanup. Application of complementary geophysical sensor systems increases the potential for discrimination of UXO targets from false alarm targets. Development of new and innovative data integration methods and cooperative geophysical inversion algorithms allows enhanced discrimination and gives potential for target classification.

1. Background

Millions of acres of former and currently used military training and testing ranges are potentially contaminated by surface and buried unexploded ordnance (UXO). The UXO exists at hundreds of sites with diverse geologic and environmental conditions, from the surface to depths as great as 10 m, and range in size from 20-mm projectiles to 2,000-lb bombs. UXO environmental remediation (UER) is required at Base Realignment and Closure (BRAC) sites and Formerly Used Defense Sites (FUDS). Active range clearance (ARC) of UXO is also required for continued safe utilization of existing facilities for training and weapons systems testing and development of future operational capabilities.

UER and ARC are two of the five DoD UXO clearance mission areas (Figure 1). Explosive ordnance disposal (EOD), humanitarian demining (HD), and countermine (CM), differ significantly in terms of operational scenarios, safety concerns, and nature of the targets (Butler 1997). However, the common threads among the five mission areas are indicated in Figure 1. False alarms, generated by geologic sources and cultural debris, necessitate excessive investigations of innocuous targets. For UER and ARC, investigations of false alarm targets (excavation) translate directly into cost. In fact, excavation of false alarm targets currently constitutes approximately 75% of total cleanup cost.

The geophysical methods most applicable to buried UXO location are magnetometry and electromagnetic induction (EMI). Magnetometry is a passive geophysical method, where the earth's natural magnetic field induces an anomalous magnetic field in buried, ferrous objects, e.g., UXO. Most magnetometer systems for field measurements, particularly in UXO surveys, are optically pumped, alkali-vapor, total field magnetometers (TFM). EMI is an active geophysical method, where a transmitter (Tx) generates a magnetic field that induces currents in subsurface conductors. The induced currents generate a secondary magnetic field that is detected by a receiver (Rx). EMI systems used for UXO surveys are predominantly time domain EMI (TDEM) systems, although frequency domain EMI (FDEM) systems are also used. For TDEM systems, the induced response of subsurface conductors is a decaying transient.

TFM and EMI are complementary in the sense that the methods predominantly detect contrasts in *different* physical properties, magnetic susceptibility and electrical conductivity, respectively. TFM and EMI are also complementary in terms of applicability/limitations and target information interpretable from measurements (Figure 2). Typical hand-held, man-portable, and towed TFM and EMI systems are shown in Figure 2. In current practice, only one of the methods (generally TDEM) is used to survey UXO sites. When both methods are used at a site, two passes over the site are required.

Following the geophysical survey, a dig list is generated showing the location of detected anomalies. Without the capability for discriminating anomalies caused by buried UXO from false alarm anomalies, all anomalies above a selected threshold must be excavated. Most survey sites will show a rapid increase in the number of anomalies as the detection threshold is lowered (Figure 3). Clearly the cost of cleanup will increase dramatically as the detection threshold is lowered, and the selection of a threshold for dig list target declaration is very subjective in practice. With no discrimination capability, all targets entered in the dig list must be excavated. Current practice requires relocation of the dig list targets with differential GPS and a confirmatory geophysical sensor.

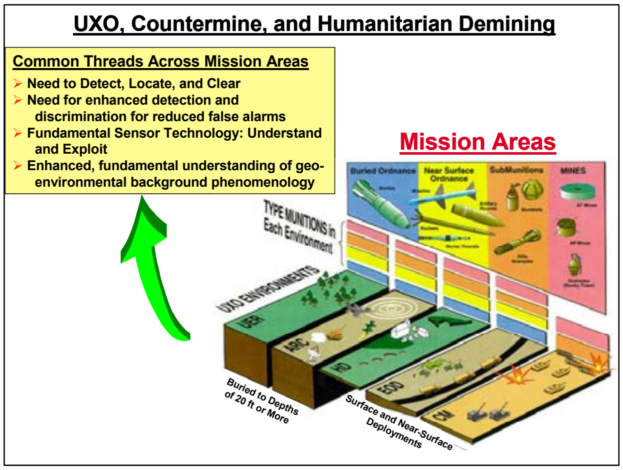

Fig. 1. Five DoD UXO clearance mission areas, illustrating Common threads

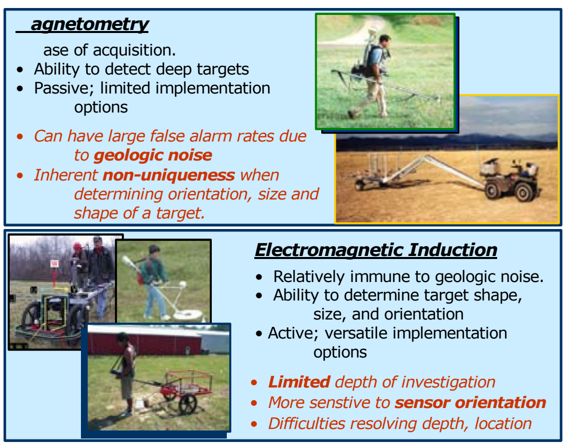

Fig. 2. Advantages and limitations of magnetometry (TFM) and electromagnetic induction (EMI).

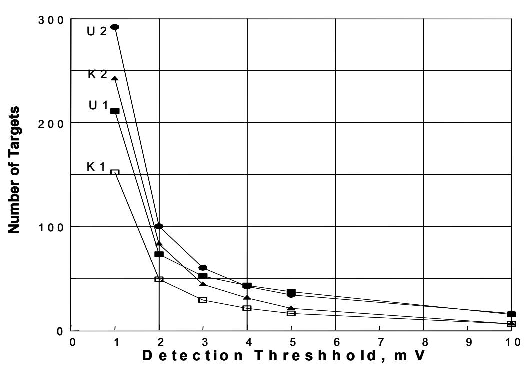

Fig. 3. Number of targets vs. detection threshold for TDEM surveys of four seeded test sites at Former Fort Ord, California.

2. UXO Detection and Discrimination Research

The Army Environmental Quality Technology UXO R&D Program of the U.S. Army Engineer Research and Development Center (ERDC) seeks to (1) develop enhanced geophysical survey systems and approaches, (2) dual-mode and multi-sensor hand-held, man-portable, and towed array systems, (3) multi-sensor data integration methods, (4) forward and inverse modeling capability for TFM, TDEM, and FDEM, and (5) discrimination and classification capability. This paper focuses on the development of multi-sensor data integration and cooperative inversion for UXO discrimination and classification. Strictly speaking, a sensor array is a "multi-sensor" system, however, in the present context, multi-sensor refers to two or more *different* sensor types either on the same platform *or* acquired in different passes over a site. A dual-mode sensor allows determination of two complementary data types from a single sensor.

3. Physics-Based Models

Geophysical surveys over a site result in two-dimensional maps of measurements of TFM or EMI response. For TFM, the map is defined by (x_i, y_j, h_{ij}), where h_{ij} is the measured magnetic intensity at the point (x_i, y_j) of the site. For TDEM, the maps are defined by (x_i, y_j, $v_{ij}(t_k)$), where the $v_{ij}(t_k)$ are measured values of the EMI transient decay at (x_i, y_j) for time t_k. Simple TDEM systems measure only one value of the transient decay (i.e., k = 1), while more sophisticated systems sample the transient decay at each location with many measurements (e.g., k = 1 to 25). Thus a TDEM map will commonly be for one value of time or for a quantity derived from the full decay transient, such as the area beneath the decay curve or a parameter characterizing the rate of decay. With the commonly used EM receiver coils (loops), the measured values are voltages. Physics-based models to calculate the induced anomalous response of a UXO buried in a geologic media must replicate the full spatial response as a function of time (or frequency for FDEM). The physics-based models can be considered "basic response models" and are commonly based on a simplified geometrical/parametrical representation of the UXO (e.g., Figure 4 and 5). While the basic response models work well for many cases, more detailed models are required to replicate the effects of UXO geometrical complexity and multiple construction materials (Butler 2004).

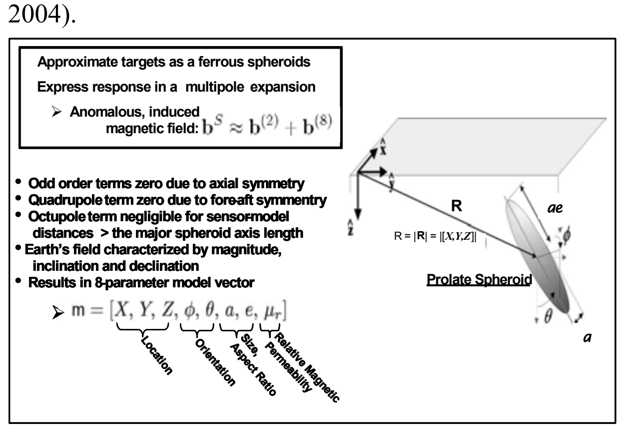

Fig. 4. Example of parametric model to simulate the induced TFM response of an axisymmetric target (prolate spheroid).

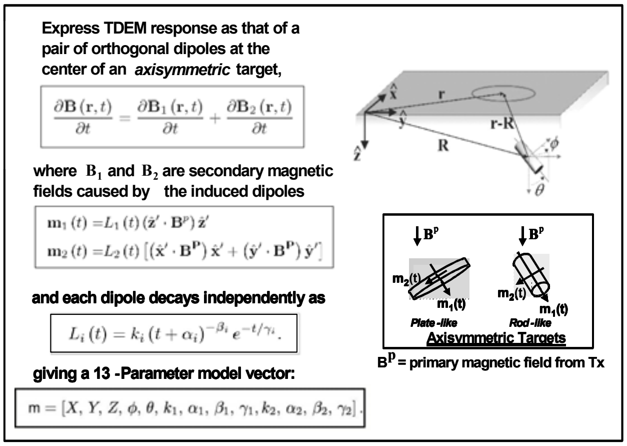

Fig. 5. Example of parametric model to simulate the TDEM response of an axisymmetric target.

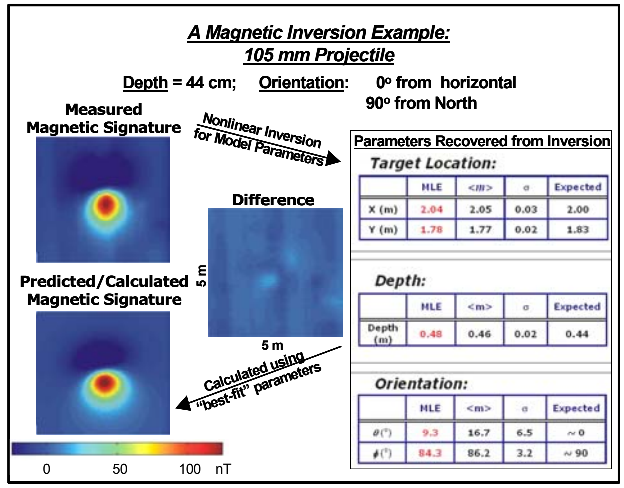

Fig. 6. Illustration of inversion of measured TFM data for model parameters (Fig. 4), where MLE is the maximum likelihood estimate of the parameters and <m> is the mean value of all estimates (Billings et al. 2002)

Using the physics-based models, measured field data are inverted using non-linear, least squares, parametric inversion procedures to give "best fitting" model parameters (e.g., Oldenburg and Li 2004). An inversion example, using the model shown in Figure 4, for the measured total field magnetic signature on a 5-m × 5-m area over a 105-mm projectile is given in Figure 6. The recovered (predicted) parameters for the location and orientation of the projectile are shown on the right side of the figure; additionally the inversion gives the recovered induced dipole moment magnitude and direction. Similarly, measured TDEM data is inverted using the model of Figure 5 to give best-fitting model parameters (e.g., for a 60-mm mortar in Figure 7). The TDEM example in Figure 7a shows the measured data and predicted (calculated) "data" using the recovered model parameters for four measurement times. Recovered model parameters, location, orientation and transient decay, are shown in Figure 7b.

4. Target Recognition: Inversion and Classification

The previous examples illustrate how TFM and TDEM data are each inverted to yield information about the parameters of a physics-based target model. Ideally, for measured TFM and TDEM data over a ferrous target, the recovered parameters will indicate compatible characteristics; for a non-ferrous metallic target, only the TDEM measurements will indicate the target. For low-noise datasets, the inversion process for both TFM and TDEM can be quite robust in terms of the fidelity of recovered parameters. However, fundamental non-uniqueness (ambiguity) and noisy data, including the effects of system noise as well as natural geological noise and cultural noise sources, are problematic for the inversion process (see limitations comments in Fig. 2). Noisy data can result in the inversion process converging to erroneous solutions, which adequately replicate the measured anomaly signature, but whose parameters aren't representative of the actual target. Effects of the fundamental ambiguity on TFM modeling and inversion

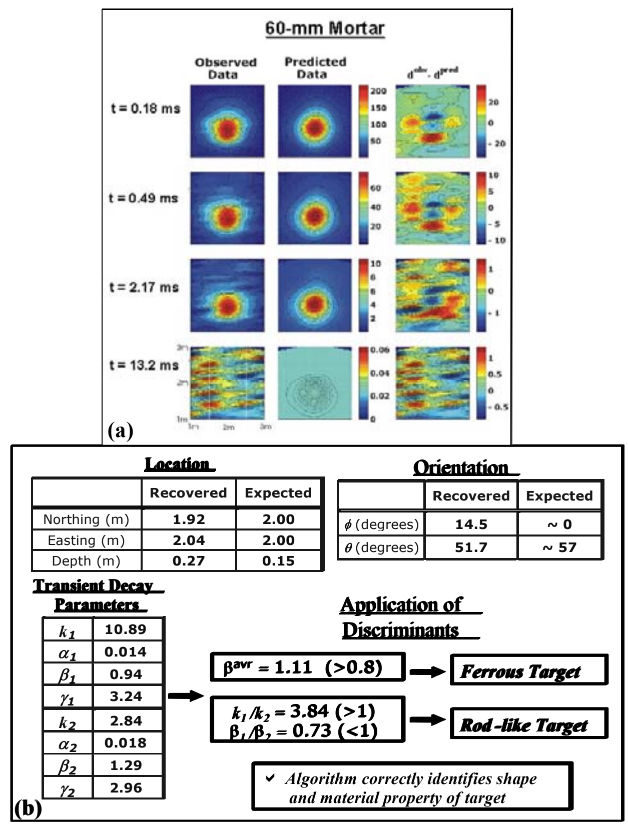

Fig. 7. Illustration of inversion of measured TDEM data over a 60-mm mortar using the model shown in Fig. 5: (a) measured and predicted data and the difference for four selected measurement times; (b) recovered model parameters (Pasion and Oldenburg 2001).

are illustrated in Figure 8, where the model of Figure 4 is used to study the induced dipoles in prolate spheroids.

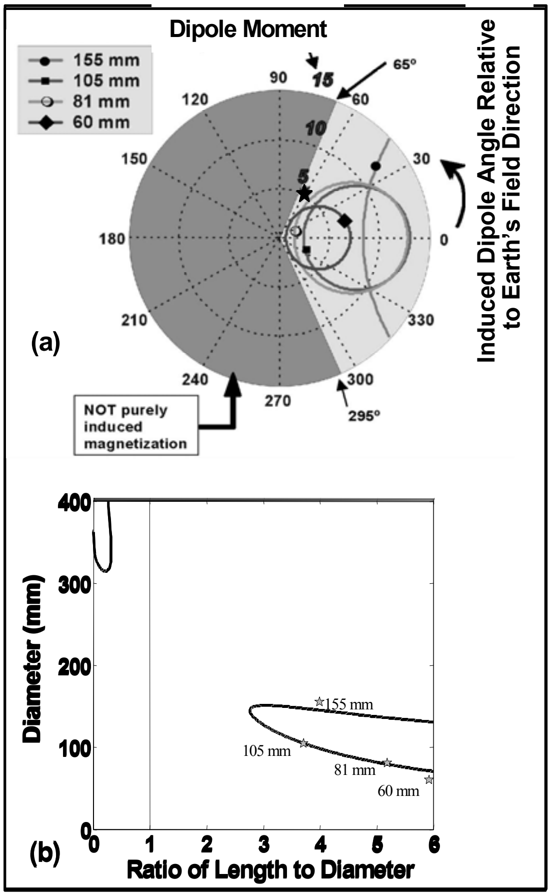

Fig. 8. Illustration of the non-unique magnetic dipole signatures of ordnance models: (a.) different sized spheroids can produce the same dipole moment; the angle of the induced dipole moment relative to the Earth's field direction is limited to < 65^0 for *purely induced magnetization*; (b.) spheroid dimensions giving the same dipole moment as 105-mm projectile at 45 deg to Earth's field.

Based on the fundamental ambiguity for TFM as shown in Figure 8, *the inversion process for TFM cannot effectively constrain the target size, shape and orientation.* However, TFM inversion is generally robust for estimating the location (x, y, depth) and the induced dipole magnitude and direction (which does not necessarily coincide with the orientation of the target model; Butler et al. 1998). Prior efforts to use inversion of TFM for target recognition involved empirical correlations between the induced dipole moment and the ferrous mass and then to the UXO item(s) having that approximate mass. Such a correlation to mass is not reliable in general, because the TFM induced dipole is proportional to the ferrous volume and not the mass (Altshuler 1996).

It is possible, however, to develop a target recognition (discrimination) approach based on the empirical observation that intact (recovered) UXO generally have no remnant (permanent) magnetization, while exploded ordnance scrap has large remnant magnetizations (Barrow and Nelson 2000). A postulated mechanism for these observations is that intact ordnance undergoes shock demagnetization during the impact process, while exploded ordnance scrap reacquires permanent magnetization through heat and pressure associated with the explosion process, in the presence of the earth's magnetic field.

Approaches for discrimination and identification using the recovered dipole moment are based on the concepts illustrated in Figure 8a. Each TFM inversion results in a dipole moment that maps to a point in the polar plot of dipole moment magnitude versus angle relative to Earth's field. The ferrous object represented by the star in Figure 8a is "closest" to the locus of possible *induced* magnetization states for the 81-mm mortar; however, it is also "close" to the curves for the 60-mm mortar and 105-mm projectile. Considering data errors, noise, and/or small remanent magnetization, the star could represent any of the three possibilities, *or* the star represents the dipole moment of a piece of ferrous scrap. The discrimination approach consists of (1) plotting all recovered dipole moments from a TFM survey in a polar plot, (2) establishing a *conservative* 75^o cone about the Earth's field direction for induced magnetization in UXO-like objects, and (3) considering recovered dipoles that plot outside the 75^o cone as non-UXO. This procedure is illustrated in Figure 9, for a FUDS site in Montana, where recovered dipoles are plotted and keyed to the results of excavation of all targets, i.e., keyed as non-ordnance and intact ordnance/large ordnance piece. Digging only those items with dipoles that plot within the 75^o cone will eliminate digging a large percentage of the non-ordnance items and will recover the intact ordnance and nearly all the large ordnance pieces. *Using the angle discriminant, all the ordnance items are recovered after digging 560 (68%) of the total of 822 targets.*

Using additional phenomenological observations as discriminants and site-specific knowledge results in even more efficient ordnance recovery for the example in Figure 9. Site-specific (historical and prior excavations) knowledge of the Montana site indicated that all ordnance items were likely 60- and 81-mm mortars and 76-, 90-, 105-, and 155-mm projectiles. The smallest possible induced magnetic moment (= 0.055 A-m^2) for spheroid models of these ordnance items is for a 60-mm mortar. *Using a dipole moment cutoff of 0.05 A-m^2 in addition to the angle discriminant results in recovering all ordnance items after digging 443 (54%) of the 822 targets.* The number of holes required to recover all ordnance conservatively includes 85 targets with poor or failed model fits in both the preceding cases.

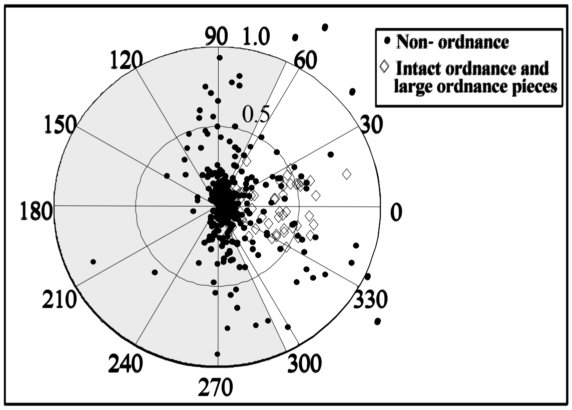

Fig. 9. Recovered dipoles from a TFM survey at a Montana site, keyed to the results of excavating *all* 822 identified targets

An additional discriminant or even ordnance identification can be based on applying a minimum remanent magnetization criterion. A remanence value is defined as the minimum distance between a recovered dipole and the induced magnetization curves for likely ordnance present at a site, expressed as a percentage of the magnitude of the recovered moment. Using the phenomenological observation that intact UXO are largely demagnetized, the results can be utilized in two ways: (1) to identify the most likely specific ordnance type for each recovered dipole (i.e., the ordnance type requiring the minimum remanence to match the recovered dipole moment for each item); (2) to rank the likelihood that items are UXO based on minimum remanence. *By including a 50% remanence cutoff discriminant, along with the angle and dipole moment discriminants, to the previous Montana example, all ordnance items are recovered after digging 402 (49%) of the 822 targets.* Billings et al. (2002) propose a formalized TFM discrimination approach based on the above concepts.

Similar problems exist for TDEM inversion relative to noisy data and fundamental ambiguity. The example in Figure 7 indicates that, for data with a high signal to noise ratio, target location and characteristics can be recovered reasonably well for the parametric TDEM model in Figure 5. Application of discriminants based on empirical observations result in classification of the target as ferrous and rod-like, and thus potentially a UXO. The discriminants are based on the recovered parameters for the two dipole-decay expressions (Figure 5):

- The value of the β*'s* correlates with magnetic permeability, such that using a threshold value of $\beta_{avg} = \{(\beta_1 + \beta_2)/2\} > 0.8$ indicates most likely a permeable target (ferrous, such as steel);
- $\beta_{avg} > 0.8 \Rightarrow$ *Ferrous Target*. If $k_1/k_2 > 1$ and $\beta_1/\beta_2 < 1$, then target is permeable and *rod-like*. If $k_1/k_2 < 1$ and $\beta_1/\beta_2 > 1$, then target is permeable and *plate-like*.
- $\beta_{avg} < 0.8 \Rightarrow$ Non-*Ferrous Target.* If $k_1/k_2 > 1$, the target is nonpermeable and *plate-like.* If $k_1/k_2 < 1$, the target is nonpermeable and *rod-like.*

For TDEM with low signal to noise ratios, the recovered parameters may indicate an incorrect location (see Figure 2) and orientation and even a misclassification of the target type, e.g., indicating a plate-like target instead of rod-like. For example, a target may be misclassified at a given depth, while it would be correctly classified at a shallower depth. The example in Figure 10 for a Stokes mortar indicates the potential for enhanced performance of discrimination and classification with TDEM by use of a location constraint. Relying on the strength of TFM for target location determination, the TDEM inversion location constraint could be provided by the TFM inversion. Such a process using multi-sensor data is termed cooperative inversion.

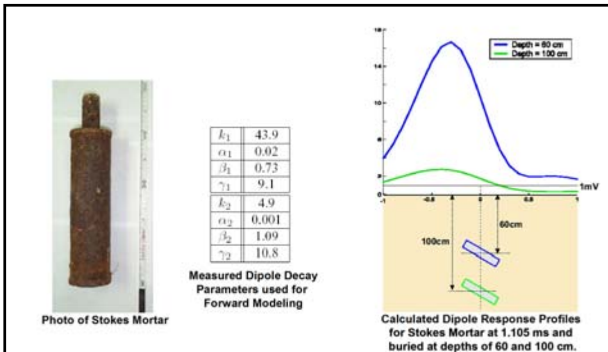

	Location X,Y (m)	Depth (m)	Azimuth (degrees)	Dip (degrees)	k_1	k_2	k_1/k_2	Interpretation
A	(0,0)	1.0	90.0	60.0	43.9	4.9	8.96	rod-like
B	(-0.01,0.00)	0.60	90.0	59.9	43.28	4.91	8.81	rod-like
C	**(-0.38,0.05)**	**0.86**	**-16.7**	**62.7**	**7.86**	**11.57**	**0.68**	**plate-like**
D	(0.01,0.00)	0.99	89.3	62.3	39.77	6.08	6.54	rod-like

Fig. 10. Example of forward modeling to predict signatures of a stokes mortar. Imposing a TDEM noise floor 0.5 mV, the table of inversion results indicates correct location and orientation recovery and classification for the 60-cm depth case (B), misclassification of the 100-cm depth case (C), and greatly improved location and orientation recovery and correct classification for the 100-cm depth case with a +/- 5-cm location constraint (D). Entry A is the correct location, orientation, and classification.

5. Target Recognition: Cooperative Inversion

Inversion is the formal process of obtaining parameters of a model that "best-fit" a set of geophysical data to the model. Similarly, joint inversion is the formal process of simultaneously "fitting" models to two or more types of independent geophysical datasets. Since the TDEM forward model (Figure 5) does not explicitly contain the spheroid dimensions and material properties, only the dipole locations and orientations are common to both TFM and TDEM models. Joint inversion has greatest potential for success when the models have a common geometrical formulation and co-located measurements for the datasets. Measurement and location errors and the number of parameters in the model vector (15) make joint inversion challenging for the TFM and TDEM datasets. If the measurements are exactly co-located, as with a dual-mode sensor system, then even with measurement errors, joint inversion is feasible. Cooperative (constrained) inversion, as described in the previous section, is a more robust process that draws on the strengths of each geophysical method (Figure 4 and 5; Pasion et al. 2004). A general cooperative inversion algorithm for TFM and TDEM datasets is illustrated in Figure 11. Target location from TFM inversion is used to constrain the TDEM inversion. The "dig/no-dig" decisions are made by application of the TDEM discriminants for targets detected by *both* sensor systems. Options exist for application of the appropriate discriminants for targets detected by only one of the methods.

6. Multi-Sensor Datasets for Cooperative Inversion and Target Recognition Capability Development

Validation and refinement of the processing flow and discrimination algorithm illustrated in Figure 11 requires high-fidelity multi-sensor datasets. Efforts to acquire the requisite datasets have included work at the ERDC UXO Test Site, the former Fort Ord, CA, and Standardized UXO Test Sites at Yuma Proving Ground, AZ, and Aberdeen Proving Ground, MD.

An example of datasets acquired at the ERDC UXO Test Site with a newly developed dual-sensor system is shown in Figure 12. The system consists of a new FDEM sensor and a TFM sensor that are rigidly mounted relative to each other, resulting in *precisely co-located datasets*. White boxes in Figure 12 indicate a target (120-mm projectile at 0.53-m depth, 0 deg azimuth, and 0 deg inclination) detected by both sensors. *The new dual-sensor system acquires both datasets in one pass over the site.*

The dual-mode sensor system shown in Figure 12 is part of the ERDC multi-sensor capability development. In addition to hand-held and man-portable multi-sensor platforms, towed multi-sensor arrays are being developed and field tested. Data acquisition with the towed multi-sensor systems is underway with formal demonstration/ validation at the Standardized UXO Test Sites. Other multi-sensor datasets acquired to support the process flow and algorithm development involve two passes over a site with the individual sensor systems.

The TDEM and TFM datasets in Figure 13 were acquired as part of a demonstration/validation at the Yuma Proving Ground, AZ, Standardized UXO Test Site. The TDEM is a new generation system that measures 26 time gates of the decaying transient, nominally over the range 180 μs – 25 ms after transmitter turn-off. The TDEM transmitter is 1- × 1-m and the three vertical component receivers are 0.5- × 0.5-m. The system is pulled through the site along profile lines spaced by 0.5 m, and making measurements along the profile lines at a rate of 10 Hz, results in measurement spacing of 10 – 15 cm. The TFM data was acquired with a 4-sensor, hand-held array of optically pumped, cesium-vapor magnetometers. Data were recorded at nominally 10-cm intervals along survey transects that were each separated by 37.5 cm. The sensors were operated at a mean ground clearance of 40-cm.

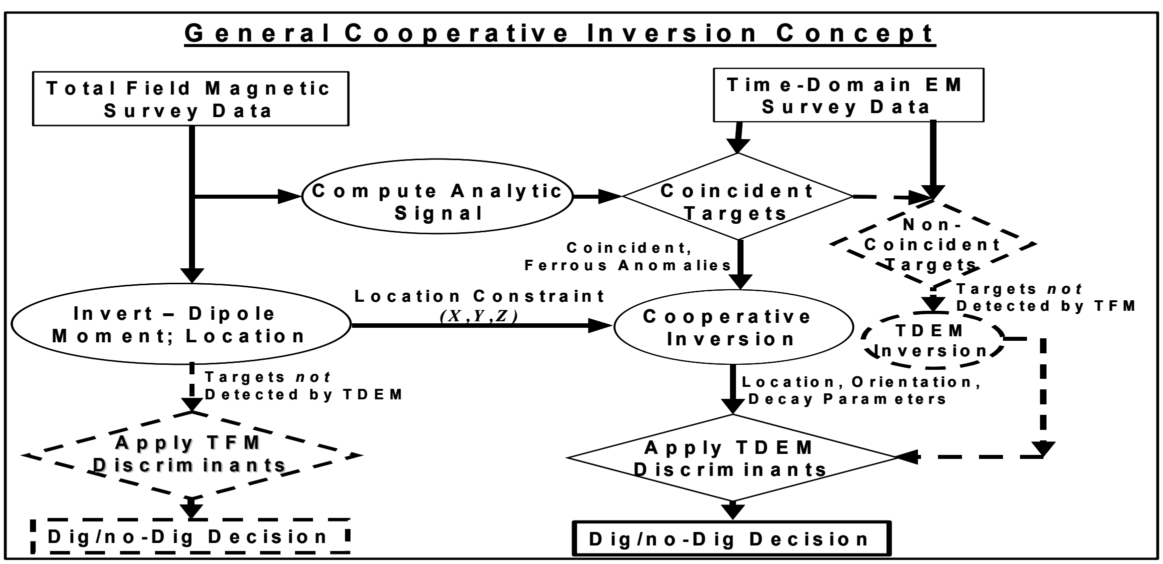

Figure 11. Concept of a process flow and general cooperative inversion algorithm, where the target location, obtained from inversion of TFM data, is constrained during inversion of the corresponding TDEM data. The processing flow allows for (1) discrimination using a location constraint during the TDEM inversion and the TDEM discriminants for targets detected by both methods, (2) discrimination using the TFM discriminants for targets detected only by TFM, and (3) using the TDEM discriminants for targets detected only by TDEM.

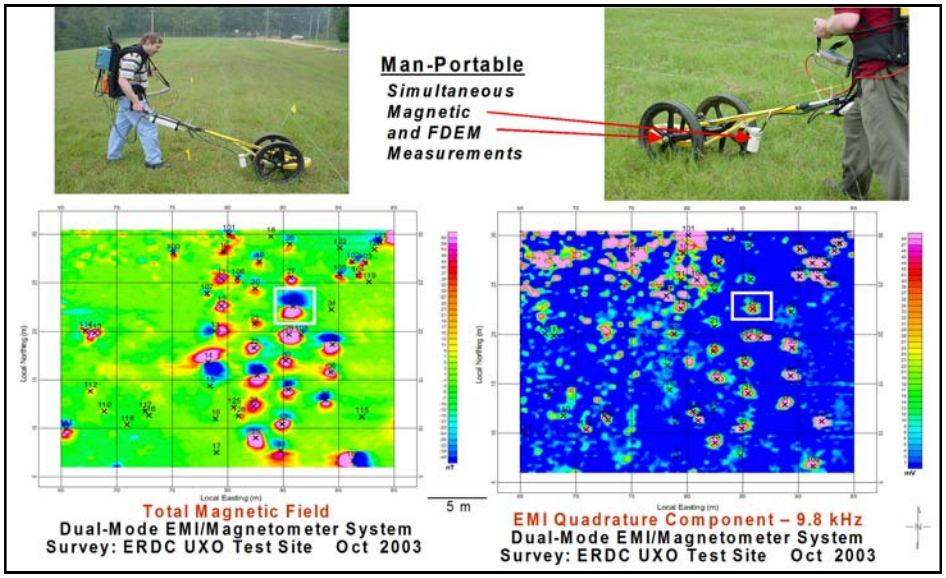

Fig. 12. New dual-sensor system (FDEM and TFM). Datasets acquired with new system at the ERDC UXO Test Site, Vicksburg, MS.

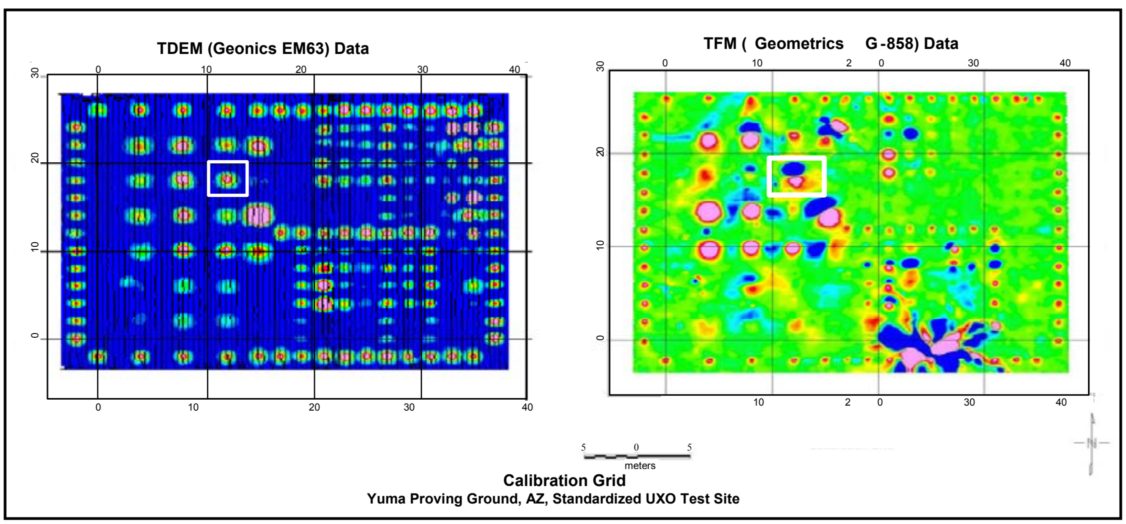

Fig. 13. TDEM (left) and TFM (right) datasets acquired on the Calibration Grid of a Standardized UXO Test Site. Each 1- × 1-m "cell" in the Calibration Grid is either empty or contains a known buried target; the known targets are either inert ordnance items or standard objects such as plates or solid spheres.

The white boxes in the two datasets in Figure 13 indicate a known target detected by both TDEM (the first time gate is plotted) and TFM. The target is a 105-mm projectile, which is oriented with the tip up at 45 deg relative to horizontal and buried at a depth of 0.4 m to the tip (shallowest part of item). For this example, the data within the white boxes is extracted and inverted for model parameters; the TFM and TDEM data are inverted separately, and then the location recovered from the TFM inversion is used to constrain the TDEM inversion (cooperative inversion). Results of the TFM, TDEM, and cooperative inversion are summarized in Figure 14. The "modeled" data panels (right) for the TFM and TDEM cases are the result of the separate inversions. The table compares the known location (Row 1) with the recovered parameters from TFM inversion (Row 2), the recovered parameters from the TDEM inversion (Row 3), and the parameters recovered from the cooperative inversion (where the location from the TFM inversion are used to constrain location in a TDEM inversion).

The recovered TDEM decay parameters give the following discriminants: β_{avg} ~ 0.8, β_1 / β_2 ~ 0.7, k_1 / k_2 ~ 2. Application of the discriminant rules given in section 4 results in classification of the target as ferrous and rod-like, although the β_{avg} parameter is somewhat uncertain for this case. In any event, the classification would result in entering the target in a dig-list for excavation.

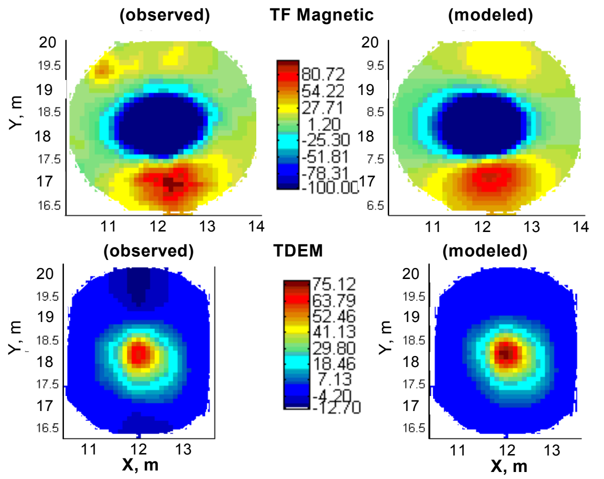

		X	Y	Z	Az	Dip
1	TRUE	12.00	18.00	0.40	0	-45
2	TFM	12.05	18.10	0.44	-7	-43
3	TDEM	12.12	18.04	0.35	-24	- 9
4	Coop	12.06	18.09	0.43	-4	-36

Fig. 14. Observed and modeled (using parameters recovered from inversion) TFM (top) and TDEM (middle) data panels (maps). Table compares known (true), TFM inversion results, TDEM inversion results, and the cooperative inversion results.

7. Conclusions and Future Work

Robust forward and inverse modeling capability for the TFM and EMI signatures of UXO have been developed. The capability is validated by application to measurements from test stands, test sites, and live sites. While separate inversion of TFM and EMI datasets works quite well in many cases, there is considerable technical justification and merit for acquiring multi-sensor datasets at UXO survey sites. Cooperative and joint inversion are two approaches for integration of the multiple datasets to produce results for discrimination and classification. Joint inversion will work most effectively when the datasets are accurately co-located and in low noise settings. Cooperative inversion, which draws on the respective strengths of the TFM and TDEM methods, is shown to allow successful inversion of TDEM to recover target orientation and discriminants even in low signal to noise settings by constraining the location (using location recovered from TFM inversion).

Future work is directed to (1) optimizing the process flow toward the goal of real-time discrimination and classification, (2) assessing the role/impact of remnant magnetization on recovered size and shape estimates, (3) incorporating remnant magnetization into the cooperative inversion process, (4) developing modeling for EMI that directly includes size and shape information to better facilitate joint inversion, (5) developing more detailed modeling capability for EMI that will account for the effects of complex geometry and multiple materials, and (6) developing classification confidence measures.

References

Altshuler, Thomas W., 1996: Shape and Orientation Effects on Magnetic Signature Prediction for Unexploded Ordnance, *Proceedings of the UXO Forum '96*, Williamsburg, VA, 282-291.

Barrow, Bruce, and Nelson, Herbert H., 2000: Analysis of Magnetic and EMI Signatures from Impacted, Intact Ordnance and Exploded Fragments," *Proceedings of the UXO/Countermine Forum 2000,* Anaheim, CA.

Billings, Stephen D., Pasion, Leonard R., and Oldenburg, Douglas W., 2002: Discrimination and Identification of UXO by Geophysical Inversion of Total-Field Magnetic Data, US Army Engineer Research and Development Center ERDC/GSL TR-02-16.

Billings, Stephen D., Stanley, John M., and Youmans, Clif, 2002: Magnetic Discrimination that will Satisfy Regulators, *Proceedings of the UXO/ Countermine Forum 2002*, Orlando, FL.

Butler, Dwain K., 1997: Round Table: Landmines and UXO*, The Leading Edge*, **16**, 1460.

Butler, Dwain K., 2004: Report on a Workshop on Electromagnetic Induction Methods for UXO Detection and Discrimination, The Leading Edge, **8**, 776-770.

Butler, Dwain K., Cespedes, Ernesto R., Cox, Cary B., and Wolfe, Paul J., 1998: Multisensor Methods for Buried Unexploded Ordnance Detection, Discrimination and Identification, Technical Report SERDP-98-10, US Army Engineer Waterways Experiment Station, Vicksburg, MS.

Butler, D., Pasion, L., Billings, S., Oldenburg, D., and Yule, D., 2003: Enhanced Discrimination Capability for UXO Geophysical Surveys, in Proc. of SPIE Vol. 5089 Detection and Remediation Technologies for Mines and Minelike Targets VIII, ed. by Harmon, Holloway, Broach, SPIE, Bellingham, WA, 958-969.

Oldenburg, D., and Li, Y., 2004: Inversion for Applied Geophysics: A Tutorial, in *Near-Surface Geophysics*, ed. by Butler, Society of Exploration Geophysicists, Tulsa, OK.

Pasion, Leonard R., and Oldenburg, Douglas W., 2001: Locating and Characterizing Unexploded Ordnance using Time Domain Electromagnetic Induction, US Army Engineer Research and Development Center ERDC/GSL TR-01-10.

Pasion, L. R., Billings, S. D., Beran, L., Oldenburg, D. D., and North, R. E, 2004: Joint and Cooperative Inversion of Electromagnetic and Magnetics Data for the Characterization of UXO, *Proceedings of the UXO/Countermine Forum 2004*, St. Louis, MO.